# Pressure Wave Attenuation Due to Anode Mufflers in Pulsed Lasers

B.N. Srivastava*
*Avco Everett Research Laboratory, Inc., Everett, Massachusetts*

**This paper addresses some new technical aspects of acoustic suppression in an open cycle pulsed laser device. An open cycle pulsed $CO_2$ laser system has been studied in order to predict the effect of various acoustic design parameters on the cavity clearing process. More specifically, the effect of an anode muffler (commonly used for transverse wave attenuation), in combination with a downstream acoustic horn, on the cavity-generated longitudinal waves is discussed by developing numerical solutions of the flow conservation equations. The results presented in this paper suggest that anode mufflers can provide an effective means of achieving rapid acoustic clearing in the laser cavity.**

## Nomenclature

$a$ = nondimensional acoustic speed ($\tilde{a}/a_0$)
$2h$ = total backing depth of the muffler
$H$ = duct height
$L$ = length of the laser cavity (cm)
$p$ = nondimensional pressure ($\tilde{p}/\rho_0 RT_0$)
$R$ = gas constant
$t$ = nondimensional time ($a_0\tilde{t}/L$)
$T$ = nondimensional temperature
$u$ = nondimensional longitudinal velocity ($\tilde{u}/a_0$)
$x$ = nondimensional longitudinal distance ($\tilde{x}/L$)
$\alpha$ = open area ratio of the sidewall muffler
$\gamma$ = ratio of specific heats
$\rho$ = nondimensional density ($\tilde{\rho}/\rho_0$)

*Subscripts*

$b$ = backing volume properties
$d$ = conditions in the main channel
$p$ = conditions in the wall perforations
$0$ = initial unperturbed conditions in the laser cavity

## I. Introduction

ACOUSTIC suppression in repetitively pulsed gas lasers is of prime technical importance due to its effect on laser beam quality and hence pulse repetition frequency (PRF). Such acoustic waves are generated in the laser cavity during the laser pumping process and are basically caused by the waste heat part of the total energy deposited in the laser cavity. The strength and nature of these waves depend on several parameters which are generally characteristics of an individual laser system. In general, two types of acoustic waves are generated in a laser cavity. The longitudinal acoustic waves (i.e., in the flow direction) are generated because the energy deposition to achieve laser pumping takes place in a small confined zone.[1] Almost invariably the energy deposition time is very short compared to the acoustic transit time across the cavity. This therefore results in an overpressure of the pumped region, causing longitudinal waves. These waves have been addressed in several recent investigations for $CO_2$,[2] chemical,[3,4] and excimer[5-7] lasers. Waves moving predominantly transverse[8,9] to the flow direction are caused by two effects. One is the nonuniform energy deposition transverse to the flow.[1] This mechanism of transverse wave generation is generally not important because any significant nonuniformity in the energy deposition is avoided by proper choice of design variables of the laser cavity.[1] Nonetheless, in some laser systems such as an excimer laser,[8] this effect may remain significant because the output laser wavelength is small ($\lambda \lesssim 0.5$ $\mu$m), implying a more stringent medium homogeneity requirement. The other mechanism of transverse wave generation is the fact that in some laser systems (such as in a $CO_2$ electric discharge laser) the electrodes are slightly displaced from the sidewalls[1] to prevent an arc from piercing the electron-beam foil. This results in almost no energy deposition between the foil and the electrode rod giving rise to strong transverse waves. Thus, a system like this would consist of strong transverse as well as longitudinal waves. To date, no work has been done to address the general two-dimensional acoustic wave suppression, due to the complexity of the problem.

This paper deals with an open-cycle pulsed laser system. Examples of open-cycle devices are $CO_2$ electric discharge lasers[2] and HF/DF chemical lasers.[3,4] In either case the approach is to place a choked orifice plate close to the laser cavity in order to achieve high PRF and mass-utilization efficiency. Thus, the longitudinal waves that travel upstream of the cavity are reflected by the choked orifice plate to a downstream location where suitable attenuators are used[2] to attenuate these waves. For transverse waves, which are generally strong for such devices, a means to attenuate these waves is needed. Since the dominant transverse wave reverberates in the laser cavity in the transverse direction between the two sidewalls, an acoustic attenuator is required in the cavity to attenuate these waves. For a laser system of the type under consideration the only space available is behind the anode rod structure.[1] Thus, conventionally, an anode absorber is used to attenuate the transverse waves. This paper concerns itself with such an anode absorber; more specifically, a finite capacity anode muffler.

There are several technical issues associated with the design of such an anode muffler. These issues are the overall effectiveness of the anode muffler in attenuating the two-dimensional waves, which consist of the transverse waves and the longitudinal waves and also management and redirection of hot gas flowing out of the muffler volume into the main channel at late times. The first of these issues could be appropriately addressed only through a two-dimensional analysis of the problem, including nonlinear effects. Although the problem is amenable to analysis through numerical calculations, the information generated from such an analysis may not provide an insight into the controlling physics and important design information. For this reason, it is considered essential to take an approach where one would introduce complexity into the problem using a step-by-step process. This stepping procedure has lead us to first analyze the problem of the effectiveness of the anode muffler in attenuating the longitudinal waves. This problem is,

Presented as Paper 81-1282 at the AIAA 14th Fluid and Plasma Dynamics Conference, Palo Alto, Calif., June 23-25, 1981; submitted July 9, 1981; revision received June 21, 1982. 

*Principal Research Scientist. Member AIAA.

therefore, the subject matter of the present paper. The objective herein is to demonstrate that the anode mufflers play a dominant role in attenuating/stretching the longitudinal wave and hence help in achieving the required medium homogeneity. Design considerations for such mufflers, therefore, must include its effect on these waves.

The effectiveness of the anode muffler in attenuating the longitudinal waves must be considered in two separate categories. When the laser initiation process takes place, the waves in the cavity consist of shocks and expansions moving upstream and downstream. If the downstream attenuators are assumed to be perfect absorbers (with no reflection), it is sufficient to estimate the effectiveness of the anode muffler on cavity-generated and flow-plate-reflected waves. However, in practice, such a perfect absorber can not be designed. Hence, the performance of the anode muffler is dependent also on what is placed downstream of the cavity. The scope of this paper is extended to the study of the anode mufflers in conjunction with downstream attenuators.

The paper is divided into several sections. Section II defines the specific problem, discusses some scale-up considerations, and identifies the requirements for the laser system. In Sec. III, we present our theoretical approach, relevant numerical analysis, and other modeling details. Section IV details the basic results of our analysis, design optimizations, and generalizations about acoustic suppression in pulsed laser systems.

## II. Physical Problem

The physical problem discussed herein relates to an open-cycle $CO_2$ electric discharge laser system. The laser gas mixture is 3/1/0.08 $N_2$,$CO_2$,$H_2$ and operates at 220 K and atmospheric pressure. These conditions have been determined from the laser kinetics and efficiency standpoint. The flow Mach number in the cavity is nearly $0.1 \sim 0.2$, while the overpressure in the cavity after energy deposition is nearly 2 atm. The cavity flow Mach number and the overpressure determine the strength of the initial waves which are required to be damped in a specified time (consistent with the desired PRF). The requirement for medium homogeneity is based on the laser beam quality and is nearly $4\text{-}5 \times 10^{-4}$. The geometry of the device consists of an anode to cathode spacing of 12.0 cm, and a spacing of 1.6 cm between foil and cathode (see Fig. 1). The physical problem identified here is basically a scaled-up version of the problem discussed in Ref. 2. This device is also discussed in Ref. 1. However, in Ref. 1, the technical problem addressed was that of the discharge and the energy deposition uniformity in relation to the laser cavity design. The problem addressed herein is the acoustic suppression studies as outlined in the previous section.

After having defined the cavity characteristics and operating conditions for the laser system, an acoustic characterization of the system is required. This characterization would enable one to determine the extent of acoustic damping that will be needed in order to achieve the required medium homogeneity within a specified time. This can be done by studying the acoustic clearing process in a semi-infinite hard wall[2] constant-area duct following the laser cavity. Figure 2 shows the results of such a study where the cavity clearing process is demonstrated with time. The dependent variables are root mean square (rms) cavity density perturbation, $(\Delta\rho/\rho_0)_{\text{rms}}$, and rms density perturbation after linear (tilt term removed) correction, and the independent variable is the nondimensional time $(a_0 t/L)$. The labels on the figure indicate various waves clearing out of the cavity. Note that the interaction of acoustic waves with the flow plate is a nonisentropic phenomenon resulting in the generation of entropy waves.[2] These waves are generally quite important because they travel with flow speed and clear out of the cavity very slowly. Ultimately, only these waves govern the cavity clearing process, although the basic cause of these entropy waves is the interaction of upstream moving acoustic waves. Therefore, an appropriate design problem is to minimize/damp these upstream propagating waves. There is yet another way to achieve the required medium homogeneity if effective damping of these waves cannot be fully accomplished. This alternative approach is to stretch the wavelength of the upstream moving wave such that it is large compared to the cavity dimension. The resulting entropy wave produced in the cavity can also be made to have wavelength that is long compared to the cavity dimension. In such a case, even though the absolute density level is high, the density distribution itself would be linear and therefore optically correctable. Further discussion of this alternative is deferred until Sec. IV. Examination of the results presented in Fig. 2 demonstrates a very slow clearing process, even after allowing for linear correction in the optics system. The acoustic clearing at about $a_0 t/L \simeq 22.0$ is achieved. This situation needs to be improved in order to achieve a higher PRF.

The preceding discussion emphasizes the need to employ suitably designed acoustic attenuators to achieve improved required PRF. Based on our previous small-scale study,[2] a possible candidate for the downstream acoustic attenuator is an acoustic horn followed by a finite capacity muffler. In the cavity a suitably designed finite capacity muffler will be employed. The characteristics of these attenuators will be established through analysis and optimization studies.

## III. Theoretical Analysis

Quasi-one-dimensional flow modeling is used in developing a theoretical basis for understanding the acoustic attenuation for the problem specified in the preceding section. The governing equations and the relevant modeling for the various elements such as flow plate, finite capacity muffler, and acoustic horn are discussed in Ref. 2, and one is referred to this for further details.

The basic discussion of this section relates to the time-dependent numerical solution of the flow conservation equations. The acoustic attenuation problem, in general, requires development of an accurate numerical scheme, because one is interested not only in strong waves at early times but also very weak waves at later times. The accuracy of the numerical scheme over a wide range of wave strengths is therefore an important issue. For this reason our numerical schemes employ "floating shock-fitting" as against "shock capturing." Also, locations of source-sink-term discontinuity[2] are treated with a local characteristics scheme to eliminate propagation of numerical errors associated with other[2] schemes. Elsewhere, a second-order-accurate MacCormack predictor-corrector scheme is used.

Numerical difficulties, however, have persisted in appropriate treatment of finite capacity sidewall muffler equations. These difficulties basically stem from two sources. First it was found that the conventional explicit schemes, such as MacCormack predictor-corrector schemes, failed to yield correct solutions when applied to muffler equations (infinite or finite capacity). This apparently happened due to the "stiff nature" of the governing equations.[10] A simple way to alleviate this problem was implemented in our previous study[2] by solving the muffler equations in characteristic form using an inverse characteristics approach. However, as one might guess, the resulting implicit scheme requires much greater computer time than the explicit schemes. The computational effort was, however, manageable for our previous work[2] due to the small-scale nature of the device. For the scaled-up device under consideration this situation became unacceptable and, therefore, further effort was devoted to devising a more efficient numerical scheme. This effort will be highlighted later on in this section.

A second difficulty that was found for this set of equations was associated with the pressure equilibrium process between the backing volume and the main channel. It was found that

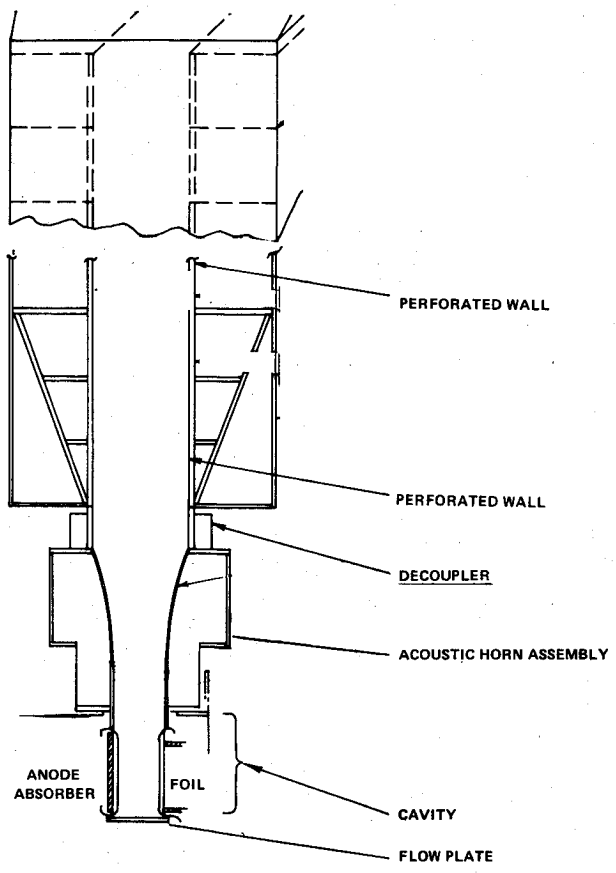


Fig. 1 Downstream flow and acoustic system.

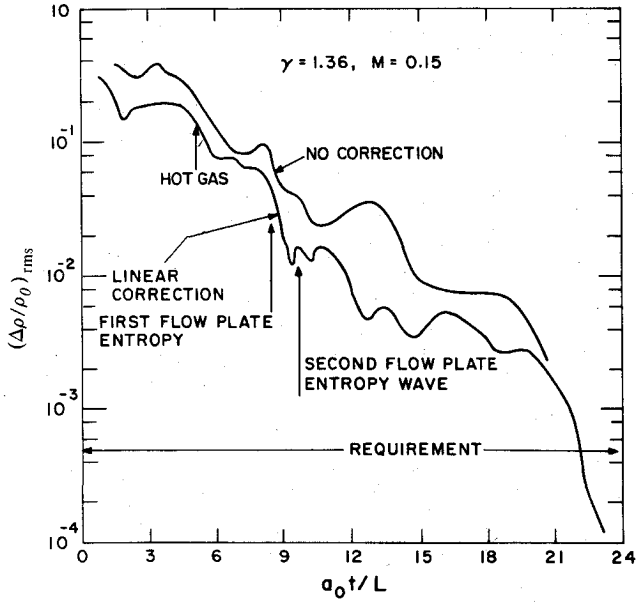


Fig. 2 Acoustic clearing with the hardwall downstream duct.

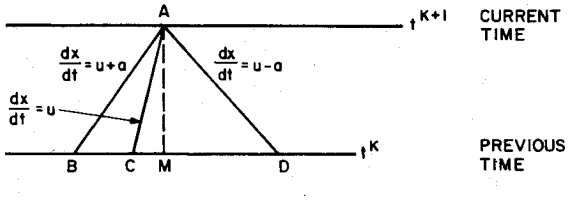


Fig. 3 Grid locations for the characteristic scheme.

when the backing volume pressure approached the channel pressure at a grid point, the iterative inverse characteristics scheme as outlined above failed to converge at that location. This situation did not cause a significant problem for the previous effort,[2] due to the small overall dimension of the system; however, for the present effort this difficulty became significant. This difficulty has been determined to be associated with the numerical error of the specific scheme being used and is caused by a relatively small mass exchange process when pressure equilibration is approached. Further discussion of this problem and its remedy follows.

**Modified Numerical Scheme**

For ease of demonstrating the numerical scheme used for solving the muffler equations, the following equations in characteristic form are presented. The equations are in nondimensional form.

$$\frac{dP}{dt} - A_P \frac{ds}{dt} + B_P - \dot{m} c_P = 0 \text{ on } \frac{dx}{dt} = u + a \tag{1}$$

$$\frac{dQ}{dt} - A_P \frac{ds}{dt} + B_Q + \dot{m} c_Q = 0 \text{ on } \frac{dx}{dt} = u - a \tag{2}$$

$$\frac{Ds}{Dt} - B_s - \dot{m} c_s = 0 \text{ on } \frac{dx}{dt} = u \tag{3}$$

Backing volume equations

$$\frac{\partial \rho_b}{\partial t} + \dot{m} C_b = 0 \tag{4}$$

$$\frac{\partial p_b}{\partial t} + \dot{m} D_b = 0 \tag{5}$$

where $P = 2a/\gamma - 1 + u$, $Q = 2a/\gamma - 1 - u$, and $s = p/\rho^\gamma$ are Riemann-invariants for the one dimensional unsteady flow. The coefficients $A_P$, $B_P$, and $C_P$ of Eq. (1), $B_Q$ and $c_Q$ of Eq. (2), $B_s$ and $c_s$ of Eq. (3), $C_b$ of Eq. (4) and $D_b$ of Eq. (5) can be determined from the conservation equations of Ref. 2 by writing the equations in characteristic form. $\dot{m}$ is the nondimensional mass exchange term.

These equations are integrated as shown in Fig. 3 at every grid point in the muffler region. All equations are written at $A$ using a first order scheme.

$$\frac{P_A - P_B}{\Delta t} - (A_P)^{K+1} \frac{(S_A - S_B)}{\Delta t} + (B_P)^{K+1} - \dot{m}^{K+1} (C_P)^{K+1} = 0 \tag{6}$$

$$\frac{Q_A - Q_D}{\Delta t} - (A_P)^{K+1} \frac{(S_A - S_D)}{\Delta t} + (B_Q)^{K+1} + \dot{m}^{K+1} (C_Q)^{K+1} = 0 \tag{7}$$

$$\frac{S_A - S_c}{\Delta t} - (B_s)^{K+1} - \dot{m}^{K+1} (C_s)^{K+1} = 0 \tag{8}$$

$$\frac{\rho_b^{K+1} - \rho_b^K}{\Delta t} + \dot{m}^{K+1} (C_b)^{K+1} = 0 \tag{9}$$

$$\frac{p_b^{K+1} - p_b^K}{\Delta t} + \dot{m}^{K+1} (D_b)^{K+1} = 0 \tag{10}$$

Unknowns are $P_A$, $Q_A$, $S_A$, $\rho_b$, and $p_b$ at time $t = t^{K+1}$. Properties at $B$, $C$, and $D$ can be determined if the foot

locations $X_B$, $X_C$, and $X_D$ are known. These are determined from the following equations.

$$\frac{X_A - X_B}{\Delta t} = (u+a)^{K+1} \tag{11}$$

$$\frac{X_A - X_D}{\Delta t} = (u-a)^{K+1} \tag{12}$$

$$\frac{X_A - X_C}{\Delta t} = (u)^{K+1} \tag{13}$$

Note that $X_A$ is known because it is a specified grid point. Equations (6-13) now represent a set of nonlinear algebraic equations. These equations were solved previously using a Newton-Raphson scheme, which involved evaluating several residuals repeatedly. This procedure was found to be inefficient for a large muffler length for which a large number of grid points are involved. Several different approaches were tried to achieve an efficient scheme. Great success was obtained by using what is classically known as "cascading approach." The procedure is outlined as follows:

1) A guess of properties at $A$ is made. This value is taken to be the same as the previous time value at the location, i.e., location $M$. This gives $P_A$, $Q_A$, and $S_A$.

2) Knowing these values, the locations $X_B$, $X_C$, and $X_D$ are determined using Eqs. (11-13).

3) A new value of $S_A$, i.e., $S'_A$, is first determined from Eq. (8) and used in Eqs. (6) and (7) to determine new values $P'_A$ and $Q'_A$, respectively.

4) Equations (9) and (10) yield, respectively, $\rho'_b$ and $p'_b$.

5) New values of $P'_A$, $Q'_A$, $S'_A$ are then tested for convergence with the old values $P_A$, $Q_A$, and, $S_A$.

6) The procedure is repeated until specified convergence criteria on all three variables are met.

The cascading approach for inviscid equations, is not generally successful.[11,12] It appears to work for this case basically because the basic equations are in the characteristic form and spatial derivatives do not appear explicitly in the differencing scheme.

In order to alleviate the second difficulty as outlined above, the mass flow term $\dot{m}^{K+1}$ is treated quite differently and is explained as follows. The expression for the mass flow is given as

$$\dot{m} = \pm \beta \rho_p u_p \frac{\mathrm{d}A_p}{\mathrm{d}x} \tag{14}$$

where $(\mathrm{d}A_p/\mathrm{d}x)$ is the nondimensional open area per unit length of the duct and is related to open area ratio $\alpha$. $\beta$ is the discharge coefficient. The upper sign is for inflow and the lower sign is for outflow. The initial computational approach with $\dot{m}$ evaluated at $K+1$ was found to fail to converge when the pressure in the main channel approached the pressure in the backing volume. A new technique was developed to treat $\dot{m}^{K+1}$ during pressure equilibration process. It can be shown that for small pressure differences the mass flux term $\dot{m}$ is proportional to the square root of the pressure differential, i.e., $\dot{m} \sim \sqrt{|p_d - p_b|}$. This means that the mass flux $\dot{m}$ approaches zero as the square root of the pressure differential. In order to avoid numerical errors associated with the pressure equilibration process, the mass flux term was expressed as

$$\dot{m}^{K+1} = \left|\left\{\frac{\dot{m}}{\sqrt{|p_d - p_b|}}\right\}^K\right| \{\sqrt{|p_d - p_b|}\}^{K+1} \mathrm{sign}\left[(p_d - p_b)^{K+1}\right] \tag{15}$$

Note that now the first term is of order one while the next two terms appropriately account for the magnitude and sign change at the current level of iteration procedure.

The application of these two new approaches for solving the muffler equations has resulted in a very efficient computational scheme for analyzing large devices where a significant part of the device consists of muffler section. The computational time for the "cascading approach" for a given problem was found to be 5-6 times lower than the previous scheme using Newton-Raphson iterative approach. This allows us to perform device tradeoff studies quite inexpensively. The total cost, however, will depend on the nature of the problem and other details required.

## IV. Results and Discussion

In this section the theoretical approach outlined previously has been used to analyze the acoustic suppression for the problem identified in Sec. II. Here basic results relating to the performance of anode muffler and downstream attenuator and their optimizations will be discussed. Foremost of these, however, is the evaluation of the acoustic performance of the scaled-up device; thus this problem is discussed first.

### Device Analysis

Figure 1 shows the basic device geometry, which was arrived at (Sec. II) by scaling our previous small-scale experiment[2] using simple scaling relations. The device consists of an upstream flow plate, followed by the laser cavity, an acoustic horn, and a finite capacity muffler. The cavity clearing process obtained from the analysis of this system is shown in Fig. 4. The results are presented in terms of $(\Delta\rho/\rho_0)_{\mathrm{rms}}$, with linear correction vs nondimensional acoustic transit time $(a_0 t/L)$. For comparison purposes, the case with the downstream hard wall duct (constant area duct without mufflers, as in Fig. 2) is also shown.

A point of interest here is to note that the performance with a hard wall downstream duct is better than that with the downstream acoustic attenuators. This situation persists until the waves reflected from the open end of the duct arrive in the cavity, which is at a later time not shown in this figure. For the hard wall case the reflected waves will be very strong because no means of attenuation exists in the duct. At short times the reflection caused by the downstream moving hot/cold interface and the impedance mismatch between the cavity and the downstream attenuator becomes important. Only the first of these is present when the downstream duct is hard wall while both are present in the later case.

This can be demonstrated more clearly by observing the magnitude of the waves that enter and leave the laser cavity for both cases. In characteristic coordinates, this can be done by plotting $P$, $Q$, and $S$ Riemann invariants at the exit of the laser cavity. This is shown in Fig. 5, where the normalized values, $\Delta P/P$, [e.g., $(P-P_0)/P_0$, where $P_0$ is the initial value], $\Delta Q/Q$, and $\Delta S/S$, are shown against nondimensional

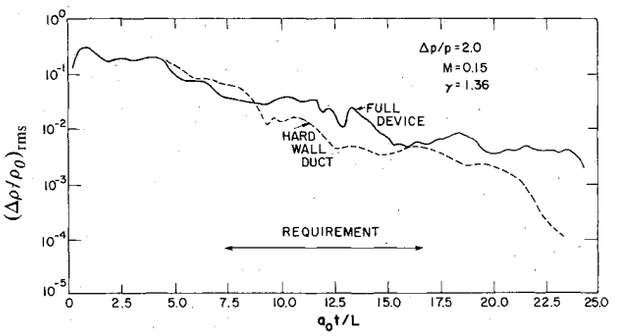


**Fig. 4 Cavity medium homogeneity with the rms tilt removed for the full device.**

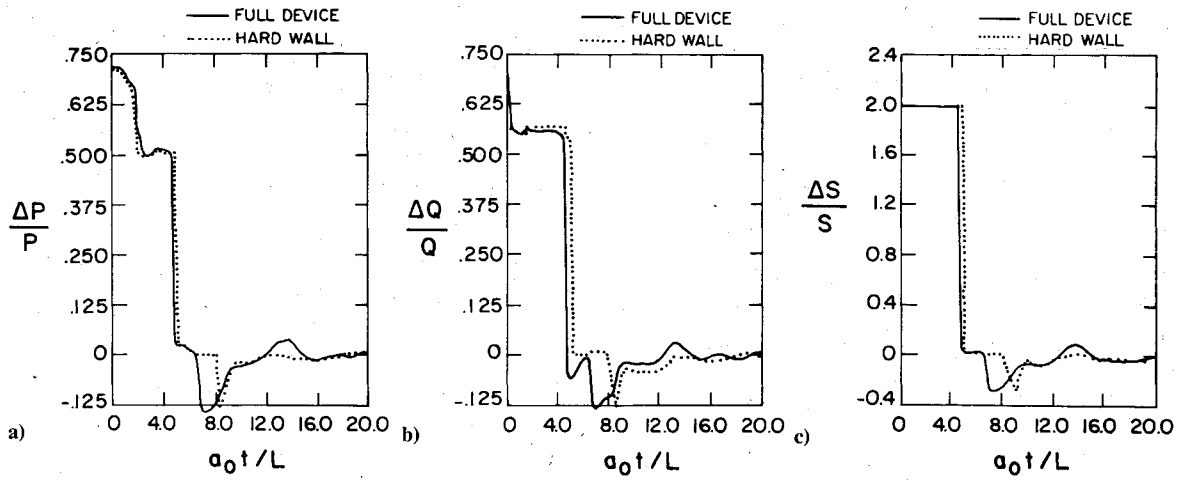


Fig. 5 Riemann invariants at the exit of the laser cavity.

time for both cases. Notice the comparatively larger magnitude of these variables for the full system as against the hard wall situation. This implies that the reflected wave magnitude is larger for the full device than that for the hard wall case. Designing the downstream attenuator duct such that the wave reflected from the hot/cold interface is either attenuated or stretched in wavelength long compared to the laser cavity and eliminating the reflection caused by the impedance mismatch between the cavity and the downstream duct is, therefore, a proper technical approach.

For short times and, as a result, for the first pulse, this objective is difficult to achieve due to two reasons. First, due to short times involved, only a few acoustic reverberations are involved and acoustic damping, which will primarily depend on the natural decay process, will be slow. (Note that only a fraction of the downstream attenuator plays any significant role in attenuation for the first pulse specifically since no attenuators have been placed in the cavity.) Second, since typical length associated with such reverberations is comparable to the cavity dimension (e.g., between flow plate and hot/cold interface or between flow plate and junction of the acoustic horn and laser cavity), wave stretching is also not achieved effectively. The result is that the overall cavity clearing process will be slow. This argument led us to believe that some sort of acoustic damping element will be required in the cavity to achieve improvement over the results demonstrated in Fig. 4. Note that this conclusion stems basically from the longitudinal wave considerations. It is this motivation that has led us to analyze the problem of pressure wave attenuation due to anode mufflers based only on the longitudinal wave considerations.

### Anode Muffler Performance

The choice of anode mufflers to achieve attenuation followed from simple considerations, as depicted in Fig. 6. The multiple reflection of the $Q$-edge wave between the hot/cold interface and the flow plate governs the ultimate clearing process, as shown in this figure. One way to achieve rapid clearing is to attenuate this wave by placing an anode muffler in the cavity.

In order to demonstrate this attenuation approach numerical calculations were performed. The overpressure considered for this calculation was nearly 1 atm. Figure 7 shows the hard wall duct calculation without any anode muffler, while Fig. 8 shows the effect of a deep anode muffler ($h/H=4.0$ and $\alpha=0.1$). The results show some interesting differences between the two calculations. First, the cavity clearing time based on $(\Delta\rho/\rho_0)$ with a linear correction of $5\times10^{-4}$ is nearly 11.0 for the case with the anode absorber,

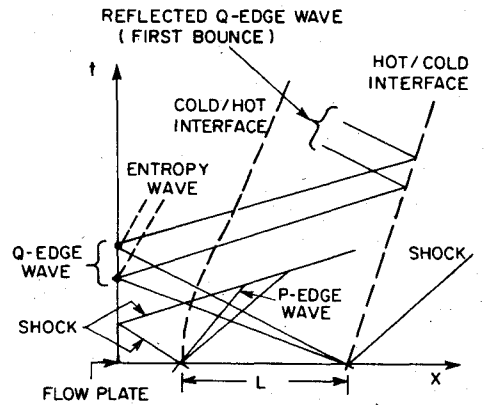


Fig. 6 Schematic of cavity waves for an open cycle laser system.

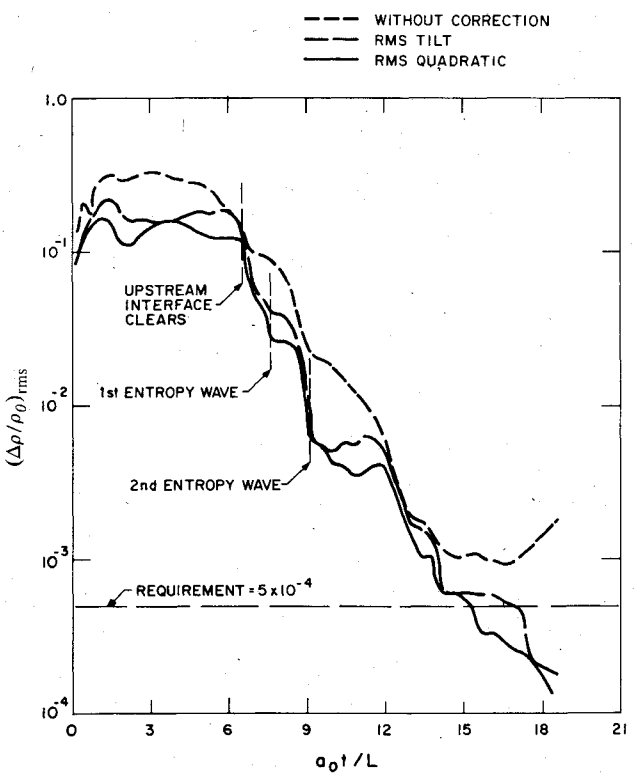


Fig. 7 Cavity flow clearing without acoustic attenuators.

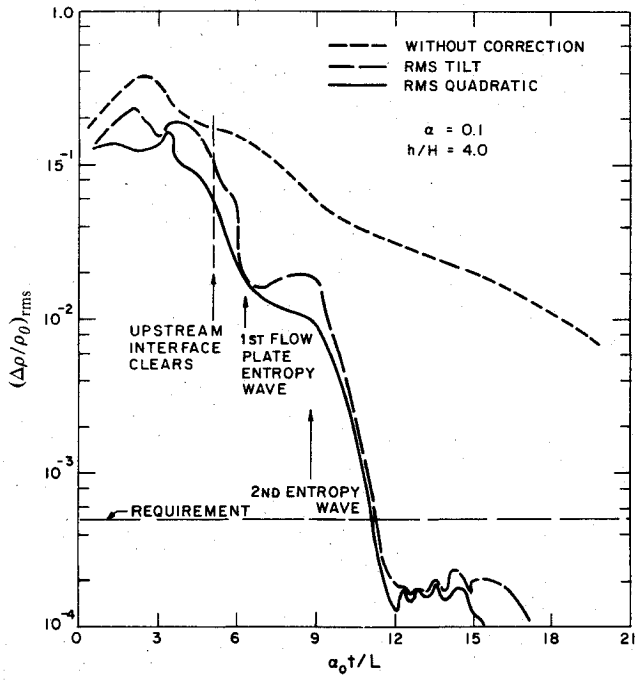


**Fig. 8 Effect of deep anode muffler on the cavity flow clearing.**

as compared to 17.5 without the anode absorber. This represents an improvement of close to 40% in acoustic clearing time for this situation. An improvement of this magnitude is considered quite high granting that the parameter values of the anode muffler were chosen arbitrarily. Second, note the difference in magnitude between $(\Delta\rho/\rho_0)_{rms}$ without linear correction and $(\Delta\rho/\rho_0)_{rms}$ with linear correction for both cases. Whereas the hard wall duct calculation (without anode muffler) does not show much difference, the calculations with anode muffler show a great difference. The value of $(\Delta\rho/\rho_0)_{rms}$ in the cavity is higher at all times with the anode muffler than without. This suggests that the density level in the cavity in the former case is higher; however, its distribution is nearly linear, so that a major part of it can be eliminated by linear correction. What is apparent from these figures is more clearly shown in Fig. 9, where $\Delta\rho/\rho_0$ is plotted in the cavity for the two cases at various acoustic transit times. Note that the scale of plot for both cases is the same except for photographic reduction. Without the anode absorber the density variation in the cavity appears to be oscillatory and noncorrectable. The effect of the anode absorber is to smooth out this oscillatory behavior. The density distribution in this case is very nearly linear. The wave stretching characteristic of the anode muffler is, therefore, used here to accomplish the required medium homogeneity. Several other studies and analyses in this area suggest that a finite-capacity muffler tends to decrease the amplitude and stretch the wavelength of an input wave. The reduction in amplitude and magnitude of wave stretching depends on the muffler characteristics.

We have performed a series of calculations to determine the effect of parameter variations on anode muffler performance for our design condition. This was done in an effort to determine an optimum configuration for the given design conditions. For this purpose, the study was limited to using a hard wall duct downstream of the cavity. Figures 10 and 11 show the effects of anode absorber depth and anode open-area ratio for this problem. These results indicate very similar performance at different parameters. However, using a bandwidth of $(\Delta\rho/\rho_0)_{rms}$ with a linear correction between 3 and $6\times10^{-4}$, one can arrive at $0.1\leq\alpha\leq0.3$ and $h/H\leq2$ as a rough estimate for optimum parameters. These parameters

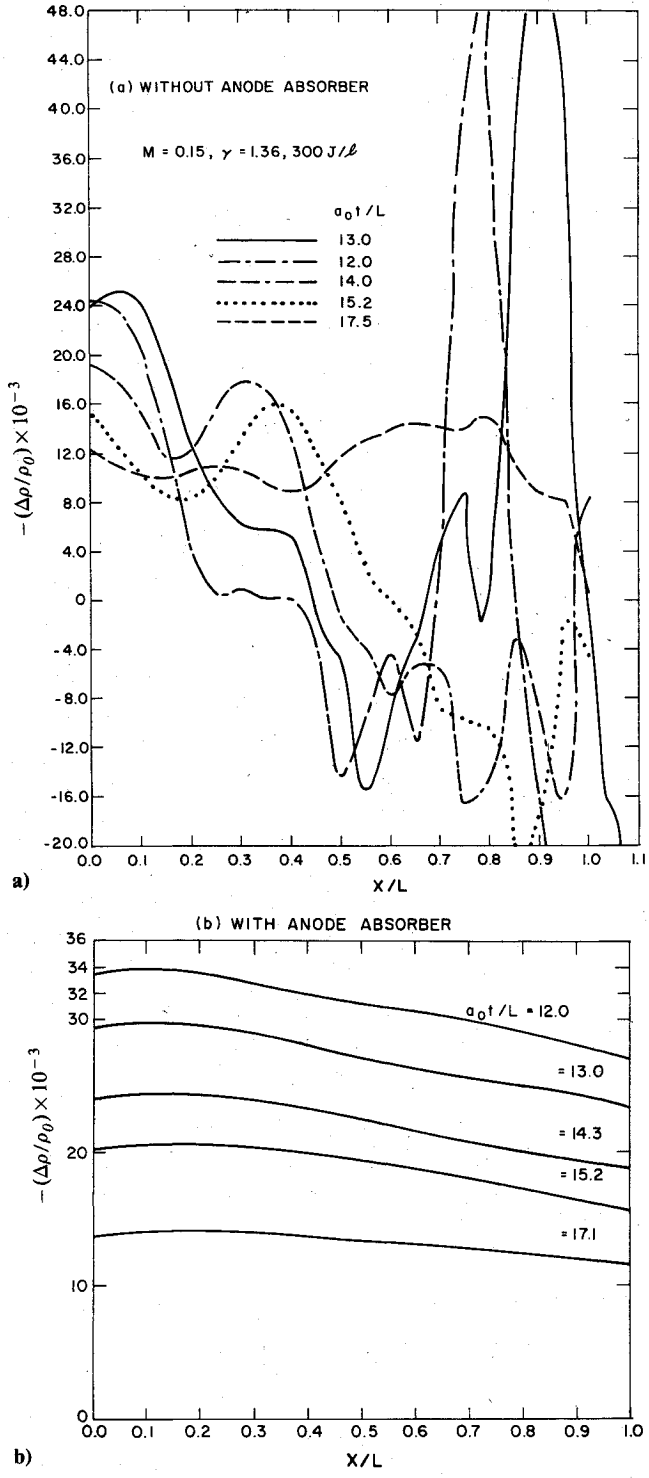


**Fig. 9 Predicted density evolution in laser cavity a) without anode muffler and b) with anode muffler.**

will be utilized further when determining the overall acoustic system at our design condition.

### Acoustic Horn Performance

The acoustic horn has been analyzed before,[2] and some evidence has been presented to demonstrate that it may have an adverse affect on the flow clearing. However, conclusive evidence to demonstrate this relative to a device has not been presented before. During this technical effort is was possible to perform simple comparative calculations to demonstrate the undesirability of the acoustic horn in laser applications.

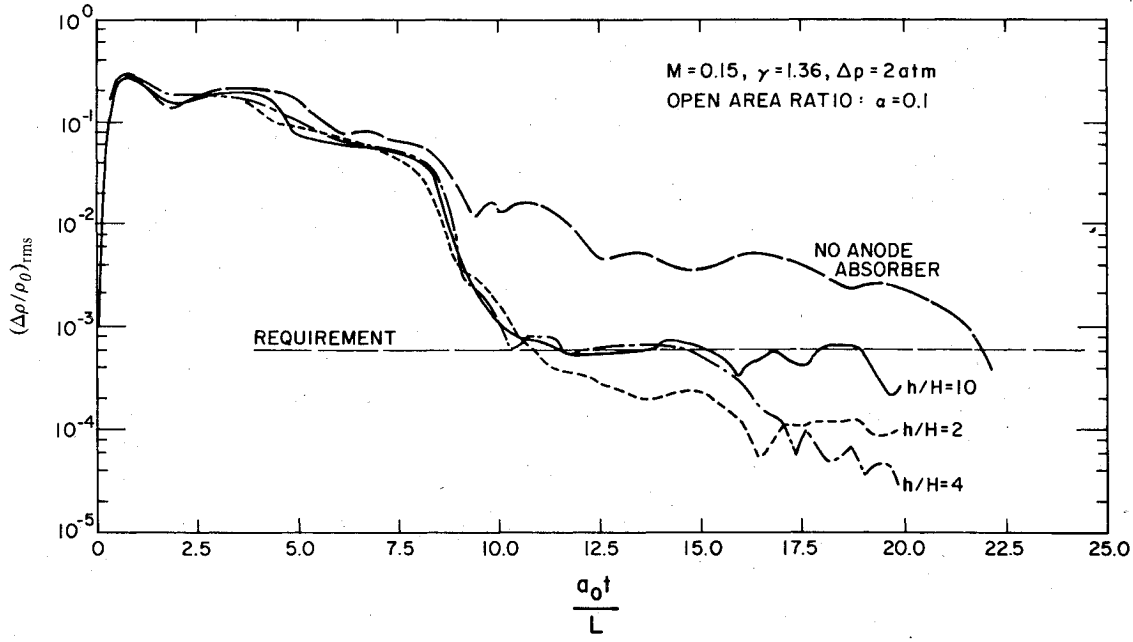


Fig. 10 Effect of anode muffler depth on the cavity flow clearing (rms tilt removed).

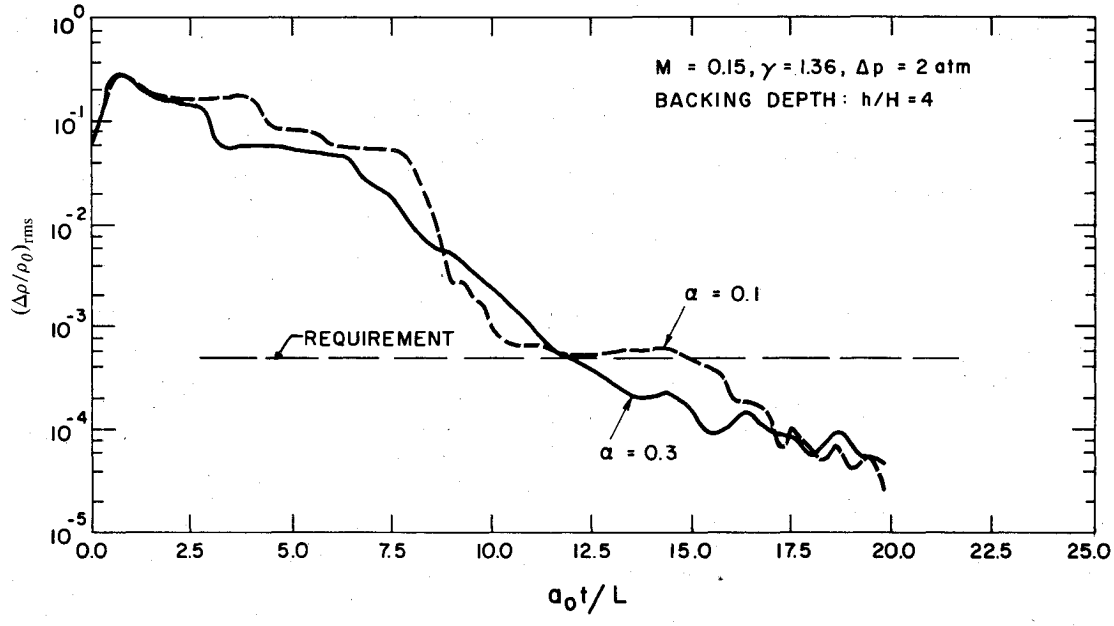


Fig. 11 Effect of anode muffler open area ratio on cavity flow clearing (rms tilt removed).

First, a simple calculation was performed for a case which included an acoustic horn followed by a straight hard wall duct as the downstream attenuator. The result of this analysis was compared with hard wall duct calculation without any acoustic horn. Notice that this type of calculation will demonstrate very clearly the effect of the acoustic horn on the flow clearing, since the difference between the two calculations represents the effect of the acoustic horn. The results of this comparison are shown in Fig. 12 as the top two curves. Once again, only $(\Delta\rho/\rho_0)_{rms}$ with linear correction has been shown. The nature of the two curves suggests that the acoustic horn tends to delay the acoustic clearing process. The disturbances reflected back into the cavity due to the acoustic horn are large enough to have a significant impact on the cavity clearing process.

In an effort to pursue this matter additional calculations were performed by including an anode muffler in the device. Two sets of calculations were made. One consisted of an anode muffler with a downstream hard wall duct; the other included an anode muffler with a downstream acoustic horn followed by a hard wall duct. The characteristics of the anode muffler were chosen based on the previous optimized study, i.e., $\alpha \simeq 0.1$ and $h/H = 2$. These results are also shown in Fig. 12, where other acoustic horn studies were presented. The results clearly show that the anode muffler is a very effective means of achieving acoustic clearing in a laser cavity. However, the acoustic horn merely tends to delay the clearing process. These results tend to demonstrate very effectively the advantage of using the anode muffler and the disadvantage of using an acoustic horn for laser applications.

### Optimum Design Study

Based on the theoretical studies presented above, it is possible to arrive at an alternate acoustic design which may be termed somewhat "optimum" in a restricted sense. The

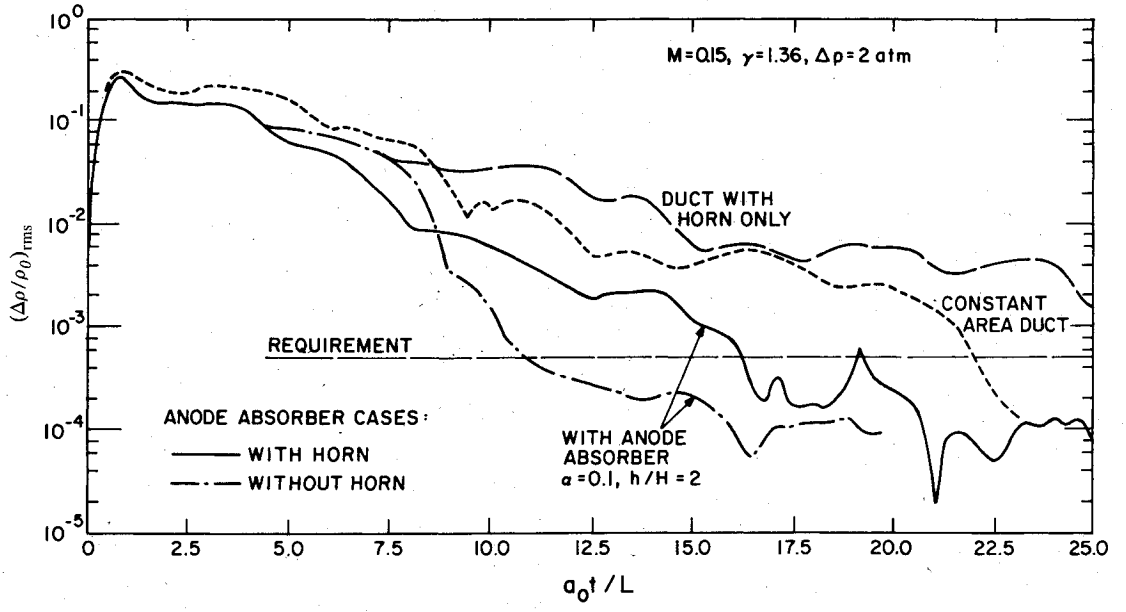


**Fig. 12 Effect of anode muffler and acoustic horn on the cavity flow clearing (rms tilt removed).**

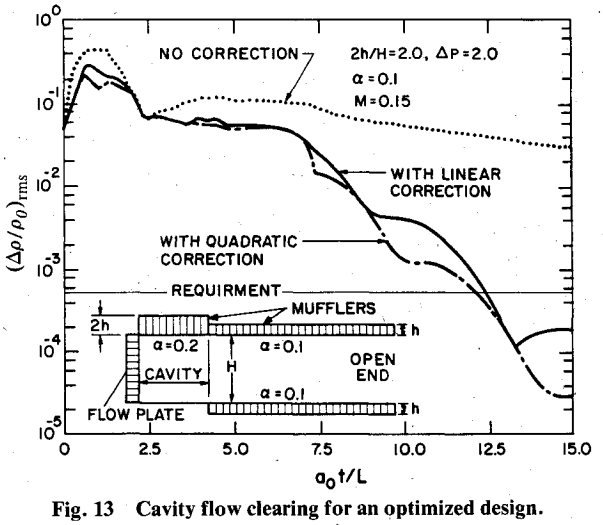


**Fig. 13 Cavity flow clearing for an optimized design.**

optimum is based on purely one-dimensional analysis, which assumes the absence of transverse waves. The present state-of-the-art does not permit two-dimensional fully nonlinear optimization/tradeoff studies, due to the complexity of the problem. Thus, an initial design has to be based on the so-called "optimum" as defined here.

For the specified design conditions, an anode muffler with an open-area ratio of 0.2 and a backing depth of $h/H=2.0$ is chosen based on previous studies. The downstream attenuator is chosen to be a finite-capacity muffler without an acoustic horn. The characteristics of this downstream muffler are specified by impedance matching with the anode muffler. Note that since the downstream muffler is used on both surfaces of the rectangular duct, $h'/H=1.0$ and $\alpha'=0.1$ (where $h'$ is the one side backing volume height in the downstream muffler, and $\alpha'$ is the open-area ratio of the downstream muffler) will ensure such an impedance matching with the anode muffler. This obviously is based on one-dimensional approach. A simple sketch of this system is shown in Fig. 13 as an insert. This figure also presents the results of our analysis for this case. Here $(\Delta\rho/\rho_0)_{rms}$ with linear and quadratic correction and without correction is presented as a function of the nondimensional acoustic transit time, $a_0t/L$. Many features of this calculation are apparent. First note that the acoustic clearing has improved from nearly $a_0t/L\simeq 28$-30 for the original case to $a_0t/L\simeq 12.5$, an improvement by a factor of nearly 2.5. Of this, a major improvement comes from the use of anode muffler and a significant improvement is caused by the deletion of the acoustic horn from the device. Second, note the effect of the linear correction on the acoustic clearing process. The cavity density appears very nearly linear at late times. The reason for this effect has been discussed before. The study reported above utilized a flow Mach number, $M$, of 0.15 in the cavity. Further analysis using $M=0.2$ shows that the clearing process improves from $a_0t/L\simeq 12.5$ to nearly $a_0t/L\simeq 9.0$, an improvement of about 30%. Thus, a proper selection of acoustic elements, their design parameters, and flow Mach number has been shown to improve the acoustic clearing time from $a_0t/L\simeq 30$ to about 9.0. This demonstrates the importance of and the need to utilize the design tools as reported here, for laser applications.

This theoretical approach toward the design of a laser acoustic system for a given specification, is by no means complete. There are several other complex phenomena such as two-dimensional wave effects, two-dimensional flow effects such as sidewall boundary layer, and jet coalescence effects near the flow plate, which have been ignored due to complexity of the problem. However, it has been also shown in previous studies[2,7,13] that the quasi-one-dimensional approach compares well with several sets of experimental data. For this reason and due to several other, more recent, comparative studies, we have determined that our computational capability provides a reasonably good prediction of the physical processes in the laser cavity. Thus, it was found unnecessary to provide further details on comparative studies but instead to demonstrate the applicability of these analytical tools towards the laser system acoustic design.

## V. Conclusions

This paper discusses some new technical aspects of acoustic suppression in an open-cycle pulsed laser device. The specific device considered is a $CO_2$ laser operating in the range $M=0.1$-0.2 and an overpressure of nearly 2 atm. The technical objective was to identify and analyze suitable acoustic suppression concepts in order to meet a specified requirement for given cavity dimensions. This goal was achieved by utilizing a computational approach where quasi-one-dimensional conservation equations are solved num-

erically to address the problem of acoustic attenuation primarily in the flow direction. A new, comparatively efficient numerical scheme has been reported and details discussed in order to alleviate some of the previous numerical difficulties encountered during the solution of the muffler equations. Application of this numerical capability is extended to study the effect of an anode muffler, an acoustic horn, and a downstream muffler on the longitudinal wave clearing process for the specified device. The results and discussion are generalized to develop an understanding and, to some extent, to develop a design philosophy for such devices. Based on these studies the following general conclusions seem relevant:

1) Anode mufflers have been shown to be very effective means of achieving cavity medium homogeneity with linear optical corrections.

2) Theoretical analysis suggests that the wave stretching concept may well be one possible solution for achieving cavity medium homogeneity with linear optical correction as against wave attenuation concept.

3) Several theoretical calculations have been presented to establish conclusively that an acoustic horn has an adverse effect on the cavity acoustic clearing process.

4) Our computational tool has led us to conclude that an appropriate design of the anode muffler and the downstream attenuator system can provide a good medium homogeneity for typical pulsed $CO_2$ lasers.

## Acknowledgments

This research was supported by the U.S. Army Missile Command, Redstone Arsenal, Alabama under Contract DAAH01-80-C-0208. Several technical discussions with Dr. C.J. Knight are appreciated.

## References

[1] Srivastava, B.N., Theophanis, G., Limpaecher, R., and Comly, J.C., "Flow and Discharge Characteristics of Electron-Beam-Controlled Pulsed Lasers," AIAA Paper 80-1433, July 1980; also *AIAA Journal*, Vol. 19, July 1981, p. 885.

[2] Srivastava, B.N., Knight, C.J., and Zappa, O., "Acoustic Suppression in a Pulsed Laser System," *AIAA Journal*, Vol. 18, May 1980, pp. 555-562.

[3] Ausherman, D.R., Alber, I.E., and Baum, E., "Acoustic Suppression in Pulsed Chemical Laser," AIAA Paper 78-237, Jan. 1978; also *AIAA Journal*, Vol. 17, May 1979, pp. 490-497.

[4] Thayer, W.J. III, Buonadona, V.R., and Sherman, W.D., "Pressure Wave Suppression for a Pulsed Chemical Laser," AIAA Paper 78-1216, July 1978.

[5] Hogge, H.D. and Crow, S.C., "Flow and Acoustic in Pulsed Excimer Lasers," AIAA Paper, Oct. 1978; also Poseidon Research Rept. 21, Feb. 1979.

[6] Tong, K., Knight, C.J., Singh, P., and Srivastava, B., "Flow and Acoustic Study for Pulsed Visible Lasers," AIAA Paper 80-0348, Jan. 1980.

[7] Tong, K., Knight, C.J., and Srivastava, B., "Pressure Wave Attenuation in Mufflers with Finite Backing Volume," AIAA Paper 79-0602, March 1979.

[8] Knight, C.J., "Transverse Acoustic Waves in Pulsed Lasers," AIAA Paper 81-1283, June 1981.

[9] Kulkarny, V., "Decay of Transverse Acoustic Waves in a Pulsed Gas Laser," *AIAA Journal*, Vol. 18, Nov. 1980, pp. 1336-1341.

[10] Roache, P.J., *Computational Fluid Dynamics*, Hermosa Publishers, Albuquerque, N.Mex., 1972.

[11] Srivastava, B.N., Werle, M.J., and Davis, R.T., "A Finite Difference Technique Involving Discontinuous Derivatives," *Computers and Fluids*, Vol. 7, March 1979, pp. 69-74.

[12] Srivastava, B.N., Werle, M.J., and Davis, R.T., "A Study of Implicit Difference Schemes for Inviscid Equations," *Computers and Fluids*, Vol. 8, 1980, pp. 413-420.

[13] Tong, K., Knight, C.J., and Srivastava, B.N., "Interaction of Weak Shock Waves with Screens and Honeycombs," *AIAA Journal*, Vol. 18, Nov. 1980, pp. 1298-1305.